Enhancing the Etch Rate at Backside Etching of Fused Silica

Klaus ZIMMER, Rico BÖHME, and Bernd RAUSCHENBACH

Leibniz-Institute for Surface Modification, Permoserstrasse 15, 04318 Leipzig, Germany
E-mail: klaus.zimmer@iom-leipzig.de

The laser-induced backside wet etching (LIBWE) technique allows straightforward etching of transparent materials such as fused silica with nanosecond UV lasers at low laser fluences. Hydrocarbon liquids are regularly exploited for LIBWE but have only moderate absorption coefficients and the etching process is affected from incubation. The estimation of the interface temperature from a simple model shows that high absorption coefficients improve the utilization of the laser energy and can result in higher temperatures exceeding the melting point. Therefore the backside etching of fused silica by means of liquid gallium using nanosecond UV laser radiation ($\lambda = 248$ nm, 25 ns pulses, 10 Hz) is investigated. A threshold fluence of about 1.5 J/cm² was estimated and etch rates close to 1 µm/pulse were measured. The square etch pits feature well-defined edges and a smooth bottom. The etch rate decreases at smaller spot size due to the thermal losses at the boundaries. The etch process involves the laser heating of gallium near the interface, the melting of the fused silica in a near surface region, and the etching of the molten layer by thermo-mechanical processes involved in laser etching.

DOI: 10.2961/jlmn.2006.03.0027
Keywords: laser, backside etching, fused silica, gallium, micromachining

1. Introduction

Laser-induced backside wet etching (LIBWE) is an indirect etching technique using pulsed laser radiation that was demonstrated first for fused silica applying a pyrene-doped acetone solution [1]. The etch rate in dependence on the processing parameters and the properties of the etched surface are studied extensively [1-7]. The complex processes of laser-induced backside wet etching that are currently not well understood in detail comprise a sequence of physical and chemical processes including laser-induced heating of the liquid and subsequently of the solid, the softening/melting of the material, and consequently the removing of the weakened material by mechanical forces due to shock waves and high pressures. Secondary effects such as bubble formation and laser-induced decomposition of the liquid also appear and probably are involved in the overall process. As all processes interact each another very complex interactions can be expected. Nevertheless LIBWE offers a high potential for high quality processing in microoptic, microfluidic, and microsystem technology. In particular LIBWE technique enables the etching micron and sub-micron structures with a high surface quality into transparent materials at low laser fluences and with a moderate etch rate [8-10].

However, the backside etching process is regularly accompanied by incubation effects [6,11], similar to laser ablation in air [12], with the result of instabilities of the etching at low fluences and pulse numbers. Further the increase of the etch rate and the reduction of the threshold fluence for prolonged etching with increasing pulse number was found. Regularly incubation processes are accomplished by alterations of the surface, e.g., defect generation and chemical surface modification. Such material modifications can change the optical properties, e.g., the absorption coefficient, as required for wide band gap materials UV laser ablation. Especially contaminations of the surface can cause an enhanced surface absorption that enables a near interface energy deposition.

Recently the backside etching process with excimer laser using gallium as absorbing liquid was demonstrated [13]. In comparison to the exploitation of hydrocarbon solutions for backside etching the process features some characteristic differences concerning the etch rate and the threshold fluence.

In this paper some recent results are presented and discussed using a simple thermal approach.

2. Experimental

The experimental set-up for laser-induced backside wet etching is described elsewhere [1,2]. A KrF excimer laser ($\lambda = 248$ nm, 10 Hz, 25 ns) incorporated into a laser workstation was used for the experiments. The laser-processing chamber was attached to a computer controlled x-y-z stage. A reflective objective (Schwarzschild, 15 x demagnification) with an optical resolution of 1.5 µm was used for projecting a square aperture with sizes from 10 x 10 µm to 100 µm x 100 µm onto the sample backside. The samples were processed with a fixed set of laser fluences (approx. 1.5 to 13.5 J/cm²) and pulse quantities (1 to 30). For the investigations fused silica samples cut from double side polished wafer with a thickness of about 380 µm and low surface roughness (< 0.3 nm rms) were used as received without additional cleaning. Pure gallium (Ga) slightly warmed up to ensure the liquid state was used as liquid absorber. After the etching process the samples were cleaned. The liquid gallium was first removed mechanically with a soft tissue. The gallium residues were wet etched with diluted hydrochloric acid. Finally all samples were cleaned ultrasonically with distilled water. The depths of the etched pits were measured with a white light interference microscope (50 x magnification). Scanning electron microscopy

(SEM) and electron probe micro analysis (EPMA) were performed after deposition of a thin gold film to the samples surface to study the topography and the chemical composition of the near surface region.

3. Results

3.1 Laser heating

The proposed mechanism of laser-induced backside wet etching is based on laser heating of the interface region up to some critical temperature that is probably near the melting point of the material to be processed. A simple estimation allows studying the influence of material parameters, e.g., the absorption length of the used liquid, referring to the maximal temperature. Fig. 1 shows schematically the thermal model of the laser-irradiated solid liquid interface equivalent to the configuration at LIBWE with the intensity attenuation of the laser beam and the resulting temperature distribution. In addition to the geometry in Fig. 1 the characteristic lengths, i.e., the optical absorption length and the temperature diffusion length, as well as the absorbed laser energy and the caloric energy for heating both materials are shown.

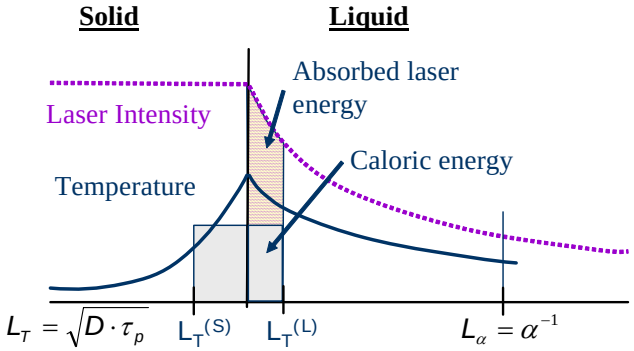

Fig. 1 Simple model for estimation the temperature in the interface region by laser heating.

To study the materials heating first the characteristic length for laser heating of the materials of matter have to be considered. In Table 1 the absorption length and the thermal diffusion length are listed for fused silica, acetone and gallium in comparison. The heating of the fused silica surface from pyrene doped acetone is optical confined in the acetone and thermal confined for the fused silica. The thermal confinement of the solid results from the surface heating by the liquid. However, there is a significant difference to the regularly discussed surface absorption of laser radiation [14].

For the estimation of the temperature a caloric approach is used wherein the respective thermal diffusion lengths limit the heated volume in both the liquid and the solid phase and the energy for heating of this volume is equal the absorbed laser energy within the limit of the heat conduction. Consequently, it is supposed that the heated volume that has a uniform temperature is limited by the thermal diffusion lengths and the laser radiation absorbed outside this volume does not contribute to the heating of the solid material. Using this approach the average temperature of this interface volume can be estimated from

$$\Delta T_{IR} = \frac{F_0 \cdot \left(1 - \exp(-\alpha^L \cdot L_T^L\right)}{\rho^S \cdot c_p^S \cdot L_T^S + \rho^L \cdot c_p^L \cdot L_T^L} \qquad (1)$$

with the laser fluence F_0, the absorption coefficient α, the density ρ, the specific heat capacity c_p, and the thermal diffusion length L_T that is defined by $L_T = 2 \cdot \sqrt{D_T \cdot \tau_p}$, with the thermal diffusivity D_T and the pulse width τ_p. The superscripts L and S denote the liquid and the solid material, respectively.

From this estimation, the influence of material properties can be discussed. With increasing heat capacity of the heated volume, either due to the material properties or due to larger thermal diffusion length, the attainable temperature decreases. Alternatively, higher absorption coefficients results in an increase of the fraction of the absorbed laser radiation that effect the heating of the interface region as long as the optical absorption length L_α is larger or similar the thermal diffusion length. Additionally, higher absorption coefficients cause energy deposition closer to the interface where the etching is accomplished.

Typical values of the optical absorption and the thermal diffusion lengths are given in Table 1 for fused silica and pyrene-doped acetone. As the absorption length of the acetone exceeds the thermal diffusion length at one magnitude, the most laser energy is not attributed to the interface heating but causes the excessive heating of a large liquid volume.

Table 1 Optical absorption lengths L_α and thermal diffusion lengths L_T of typical material.

Material	L_α [m]	L_T [m]
Fused silica	>> 1	$2.5 \cdot 10^{-7}$
Acetone (Py)	~$1.2 \cdot 10^{-6}$	$8.3 \cdot 10^{-8}$
Gallium	< $1 \cdot 10^{-7}$	$1.7 \cdot 10^{-6}$

According to equation (1) the surface temperature for a laser fluence of 0.7 J/cm² was estimated using the above mentioned parameters and the material properties of fused silica and acetone to be about 960 K. However, the melting temperature of fused silica with T_M = 1983 K is much higher than the calculated temperature.

As the absorbed laser energy directly influences the achievable temperature a reduction of the absorption lengths causes higher temperatures [15]. Using a surface absorbing liquid material such as liquid gallium the whole laser energy is absorbed near the solid liquid interface and much higher temperatures can be achieved at the same absorbed laser fluence even though the thermal conductivity of metals is much higher than that of hydrocarbon solutions (see Table 2). The temperatures that can be calculated with equation (1) exceed, as shown in Table 2, the melting point of fused silica, so that etching of a molten layer is probable. Of course, the temperature increases with rising laser fluence further. It should be noted that at the same absorbed laser fluence clearly different temperatures can be achieved using either hydrocarbon or metallic absorber.

Table 2 Comparison of the estimated temperatures at the fused silica liquid interface for two types of absorber.

System	F_{Typ} [J/cm²]	$(1\text{-}R)\cdot F$ [J/cm²]	ΔT [K]
Fused silica / Acetone (Py)	0.7	0.68	~960
Fused silica / Gallium	3.0	0.69	~2050

To study experimental the exploitation of highly absorbing metallic liquids for backside etching the etch behavior of fused silica using gallium as liquid was investigated.

3.2 Backside etching with gallium

A characteristic etch pit achieved by laser-induced backside wet etching of fused silica using liquid gallium as absorber is depicted in the SEM image of Fig. 2 a). The depicted square pit was etched at a laser fluence of about 4.5 J/cm² applying 30 pulses and demonstrates exemplarily that the etched pits have well-defined edges and a smooth bottom. A surrounding region of some micron width outside the etched pit with a higher roughness was observed where a small amount of gallium was found as EPMA measurements reveal. Contrary to that, at the bottom of the etched pits and the virgin surface area that were also in contact with the liquid gallium no Ga-signal was found. Interference microscopic measurements show in addition that the surrounding rough area is higher than the virgin surface i.e. material is redeposited.

High laser fluences and high pulse numbers that results in deep etched holes cause crack formation and the shell-like bursting of the surface at or near the etched regions at the larger spot sizes. Such effects were also observed at hydrocarbons LIBWE of brittle material such as fluorides. However, as the etch rate achievable in gallium LIBWE is approximately 30 times higher than for hydrocarbon LIBWE much higher pressures and stronger shock waves can be expected. Therefore, the tendency for crack formation is more pronounced when gallium is utilized for etching.

The roughness of the etch pit bottoms was measured by AFM and yields a value of 45 nm rms at an area of 10 µm x 10 µm. Compared to the virgin surface the substantial higher rms value can be divided in a waviness and a high spatial frequency part. After mathematical removing of longer waviness by 0.2 µm cut-off filtering a probable process inherent roughness of 7 nm rms was calculated that approximates typical values found for backside etching with liquid hydrocarbons, too [14]. The waviness can originate from the fluence distribution as the laser fluence directly influences the etch depth or from specific processes associated with etching. As the melting of the materials surface can be suggested during the etching, hydrodynamic processes can be responsible for this waviness in addition.

The depth of the etched pits increases linearly with the pulse number up to the maximum applied quantity for all investigated laser fluences. In addition, etching with the first laser pulse was observed also for low laser fluences slightly above the threshold fluence. These characteristics of the etching process refer to negligible incubation processes.

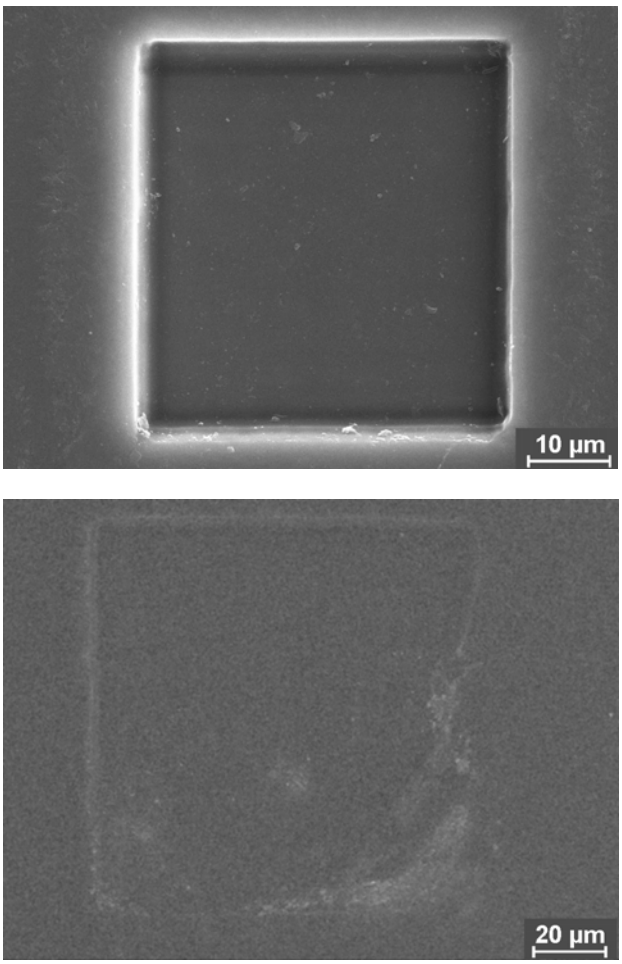

Fig. 2 SEM images of a square sized etch pits: a) Typical etch pit with a size of 50 x 50 µm² etched into fused silica with 30 pulses at a laser fluence of 4.5 J/cm² and b) a characteristic surface processed with a 100 x 100 µm² sized mask and a laser fluence between the first and the second etch threshold.

The laser fluence has the most important effect on the etch rate of fused silica. In Fig. 3 the etch rate in the fluence range from 1.3 to 8 J/cm² gallium is presented. The shown etch rates that were determined from the measured final etch depth of etch pits were averaged over all applied pulse numbers. A first threshold of about 1.3 J/cm² can be extrapolated from the slope of the linear etch rate fit that is shown as a straight line in Fig. 3, too. A second threshold fluence occurs at a laser fluence of about 2.5 J/cm² after that the etch rate increases approximate linearly as the sketched line of Fig. 3 proves. The reasons for the comparable high threshold fluences are the high reflectivity (~80 %) and the high thermal conductivity (~300-times of hydrocarbons) of metallic gallium.

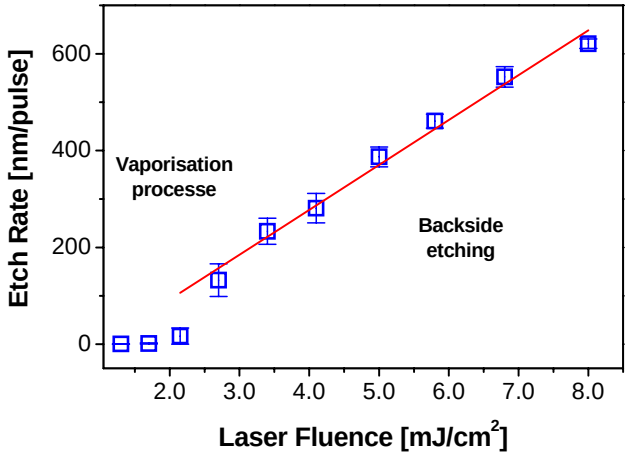

Fig. 3 Etch rate of fused silica calculated from square etch pits with a size of 100 x 100 µm². The etch rat was averaged over all applied pulse numbers from 1 to 30.

The impact of the laser fluence on the quality of the etched surface is less in comparison to hydrocarbons once the second threshold is exceeded. However, below the second fluence threshold only uneven, rough and not well bordered patterns were observed as Fig. 2 b) shows. Therefore, this fluence range is not favorable for defined materials etching.

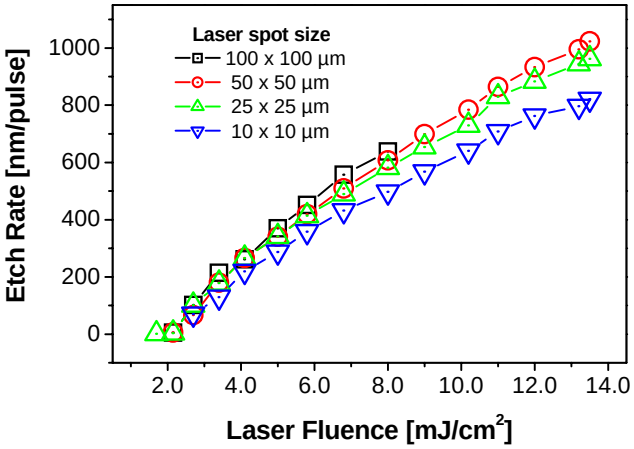

Fig. 4 Spot size dependence of fused silica etch rate at LIBWE with gallium for 3 laser pulses. The tendency of etch rate decreasing with size reduction is clearly.

The spot size dependence of the etch rate that is depicted in Fig. 4 shows the tendency of the etch rate reduction at reduced spot size. A similar behavior was observed at backside wet etching with hydrocarbons, too [6]. However, the reasons for the size dependent rate reduction might be different due to the different material properties and various processes involved in etching. In gallium backside etching the surface modification due to decomposition products or contaminations should be less important due to the high absorption coefficient of gallium that cause a near interface laser absorption so that near solid surface material alteration with enhanced laser absorption should be less influence the overall process. Additionally, the size dependence of the etch rate is opposite to the results obtained at nanosecond laser ablation, e.g., of polymers in air, where the etch rate increases with decreasing spot size [16,17]. In this case the reasons for the enhanced ablation rate with reduced spot size are the less interactions of the nanosecond laser pulse with the ablation plasma resulting in the absorption or scattering of the laser radiation. Therefore, both explanations can be ruled out.

Hence, due to the high thermal conductivity of metals the non-irradiated surrounding areas were heated in addition. With reduced spot size the ratio for heating the surrounding areas increase and should result in a reduction of the temperature. Consequently, the thermal problem becomes 3-dimensional and energy dissipation increases with smaller spot sizes.

4. Discussion

Threshold fluence for etching of fused silica with gallium is comparatively high in comparison to LIBWE with hydrocarbon solutions [3,6] but significantly lower than for laser ablation on air [12]. The reasons of the higher threshold fluences are the higher reflectivity of the fused silica gallium interface and the much higher thermal conductivity. Considering the absorbed laser fluence (compare Table 2) backside etching with hydrocarbons and gallium features nearly the same experimental threshold. Further, comparing the estimated temperatures the usage of gallium results in a higher temperature as the laser energy is absorbed completely near the materials interface.

The negligible incubation processes of the gallium LIBWE are a special characteristic of this high rate process. However, this does not imply that the etched surface do not suffer material alterations. As the EMPA investigations show in the vicinity of the etch pits little contaminations are found. Further, the melting of the surface also induces material changes due to the fast cooling rate after the laser pulse. Therefore, material alteration can probably be expected but they does not influence the etch process very much. Even alterations of the optical material properties have only little impact as the high absorption of the gallium causes a nearly complete surface absorption of the laser radiation so that material alteration of the interface does not influence the process.

The comparison of the second threshold with the estimated temperatures and the melting point of fused silica show a good coincidence. Therefore, it can be assumed that melting of the material accompanies the etch process. Once the material is molten, mechanical forces easily accomplish the removing of the material.

The modified appearance of the surface processed with laser fluences between the first and the second threshold probably refer to near surface material modifications as the locally different secondary electron emission (shown in the image as brighter areas) let guess.

Furthermore, the thermal model predicts a linear temperature rise with increasing laser fluence. As with increasing interface temperature the molten depth increases too the nearly linear rise of the etch rate can be associated to the increase of the melting depth.

The spot size dependence of the etch rate can as shown also be interpreted in terms of the model.

The redeposited material surrounding the etch pits with the included gallium contaminations gives rise to the conclusion that parts of the molten fused silica are stepwise redeposited and during the step by step redeposition gallium contamination occurs at the interfaces.

Hence, the etching process is principally thermal driven whereat higher fluences results in higher melting depths and therefore higher etch rates.

5. Conclusion

The backside etching of fused silica using gallium as typical material of a new class of liquid absorber is successfully demonstrated. The etch process features a comparable high etch threshold of 1.3 J/cm² due to the high reflectivity and the high thermal conductivity of gallium but enables etch rates of approx. 1 µm/pulse.

The linear rise of the etch depth and the etching with the first pulse show that only minor incubation processes are present. As alterations of the material can be expected as a consequence of the high etch rate and the proposed melting of the surface during etching the reason of the minor incubation effects observed is the high absorption coefficient of gallium that screens the effects of material modifications at the near surface region.

From the achieved results, it can be concluded that a thermal mechanism dominates the etching. It is proposed that the main processes of laser etching comprise laser heating of gallium, the melting of the near surface region up to a depth similar to the etch depth, and the ejection of the molten material by mechanical forces also involved in pulsed laser processing.

The material properties of gallium that are basically distinctive to that of hydrocarbons are accountable for the specific characteristics of this new etch process. These properties especially the high absorption of gallium enables probably the extension of backside etching with respect to additional materials and the exploitation of further laser sources. In particular well-developed and industrial proven ns lasers with wavelengths in the IR and VIS range can be applied. With the usage of IR lasers, e.g., Nd:YAG lasers, the processing of further materials is enabled.

Acknowledgement

The authors are grateful to Ph. Hadrava for the help in the experimental work. The skilled AFM measurements of D. Hirsch are acknowledged. This work was financially supported in parts by the Deutsche Forschungs-gemeinschaft Germany under contract DFG ZI660/5.

References

[1] J. Wang, H. Niino, and A. Yabe: Appl. Phys. A **68** (1), (1999) 111.

[2] R. Böhme, A. Braun, and K. Zimmer: Appl. Surf. Sci. **186** (1-4), (2002) 276.

[3] H. Niino, Y. Yasui, X. M. Ding, A. Narazaki, T. Sato, Y. Kawaguchi, and A. Yabe: J. Photochem. Photobiol. A **158** (2-3), (2003) 179.

[4] C. Vass, T. Smausz, and B. Hopp: J. Phys. D **37** (17), (2004) 2449.

[5] G. Kopitkovas, T. Lippert, C. David, S. Canulescu, A. Wokaun, and J. Gobrecht: J. Photochem. Photobiol. A **166** (1-3), (2004) 135.

[6] R. Böhme and K. Zimmer: Appl. Surf. Sci. **247**, (2005) 256.

[7] Y. Kawaguchi, X. Ding, A. Narazaki, T. Sato, and H. Niino: Appl. Phys. A **80** (2), (2005) 275.

[8] K. Zimmer, R. Böhme, A. Braun, B. Rauschenbach, and F. Bigl: Appl. Phys. A **74** (4), (2002) 453.

[9] X. Ding, Y. Kawaguchi, T. Sato, A. Narazaki, R. Kurosaki, and H. Niino: J. Photochem. Photobiol. A **166** (1-3), (2004) 129.

[10] R. Böhme, J. Zajadacz, K. Zimmer, and B. Rauschenbach: Appl. Phys. A **80**, (2005) 433.

[11] Y. Yasui, H. Niino, Y. Kawaguchi, and A. Yabe: Appl. Surf. Sci. **186** (1-4), (2002) 552.

[12] J. Ihlemann and B. Wolff-Rottke: Appl. Surf. Sci. **106**, (1996) 282.

[13] K. Zimmer, R. Böhme, and D. Ruthe: "*Backside laser etching of fused silica using liquid gallium*", Appl. Phys. A (2006), *accepted for publication*.

[14] D. Bäuerle: *Laser Processing and Chemistry, 3. Ed.* (Springer, Berlin, Heidelberg, New York, 2000).

[15] C. Vass, B. Hopp, T. Smausz, and F. Ignácz: Thin Solid Films **453-454**, (2004) 121.

[16] M. Eyett and D. Bäuerle: Appl. Phys. Lett. **51** (24), (1987) 2054.

[17] H. Schmidt, J. Ihlemann, B. Wolff-Rottke, K. Luther, and J. Troe: J. Appl. Phys. **83** (10), (1998) 5458.

(Received: May 16, 2006, Accepted: November 20, 2006)